THE UNIVERSE IN THE LIGHT OF LHC

M. Krawczyk, M. Matej, D. Sokołowska, B. Świeżewska

Faculty of Physics, University of Warsaw
Pasteura 5, 02-093 Warszawa, Poland

(Received December 30, 2014)

The Large Hadron Collider (LHC) provides data which give information on dark matter. Especially measurements related to the Higgs sector lead to strong constraints on the invisible sector which are competitive with the astrophysical limits. Some recent LHC results on the dark matter coming from the Higgs sector in the Inert Doublet Model (IDM) are presented.

DOI:10.5506/APhysPolB.46.169
PACS numbers: 12.60.Fr, 14.80.Ec, 14.80.Fd, 95.35.+d

1. Introduction

In the fall of the year 2014, one can safely conclude that the SM-like Higgs scenario [1–3] is being observed at the LHC [4, 5]. Such scenario can be realized in various models beyond the Standard Model (SM). It was found recently that the LHC is very effective in constraining models with the so-called Higgs-portal to the dark matter (DM), see *e.g.* [6]. In particular, LHC results on the Higgs boson properties can give stronger limits on the Higgs–DM couplings than the astrophysical DM experiments. In addition, some important constraints are coming from the dedicated search of dark matter at the LHC [7].

Let us start with a little bit of history. It was only 50 years ago when the Quark Model as well as the mass generation mechanism was proposed. These were crucial steps towards building a theory of elementary particles known as the Standard Model. The first idea of a global SU(3) symmetry arose from an observation and a classification of plethora of hadrons, which were being discovered copiously in early 1950s. It led to our current understanding of the structure of matter at the fundamental level, probed up to a distance of 10^{-18} cm, in form of 3 generations of quarks and leptons.

The masses of these particles show no clear pattern, besides the fact that second generation of fermions is heavier than the first one, and the third one is the heaviest. Among the particles which are carriers of the fundamental interactions, the photon (electromagnetic interaction) and the gluons (strong

interaction) are massless, while W and Z, the carriers of the electroweak force, are massive, actually very massive as compared to the proton. It was already known in the 1960s that this may create a serious problem in describing a very short range weak interaction (a point-like interaction according to Fermi) in theoretical approach based on a local symmetry.

1.1. Brout–Englert–Higgs mechanism in the SM

The Brout–Englert–Higgs mechanism (BEH), proposed already in 1960s, is based on spontaneous breaking of the EW symmetry SU (2) × U(1) to $\mathrm{U(1)_{QED}}$ [1–3]. One SU(2) doublet Φ of spin 0 fields with a non-zero vacuum expectation value v (VEV) is introduced, and the gauge bosons and fermions acquire mass thanks to interaction with this constant field component. Mass of $W^{\pm}$ generated this way is equal to $M_W = gv/2$, and at the tree level $\rho = \frac{M_W}{M_Z \cos\theta_W} = 1$. Masses of fermions are generated due to the Yukawa interaction with Φ.

The Higgs boson h which arises in the BEH mechanism has spin 0, even CP parity and no electric charge. Its couplings to the SM particles are all fixed, being proportional to their masses. The only unknown parameter is (was) M_h related to the strength of Higgs self-interaction. Long term hunting for a Higgs boson seems to have reached its finale in the summer 2012, when at the LHC the Higgs boson with mass around 125 GeV was discovered. Up to now, with all the collected data (already 1 million of Higgses!), the signal strengths in various channels (defined with respect to the SM prediction) are close to 1, and the observed scenario can be described as an SM-like Higgs scenario.

1.2. SM-like Higgs scenarios at the LHC

Although the SM is in very good agreement with the existing data, there are many serious arguments to go beyond it. The SM has many free parameters, contains massless neutrinos, does not have a DM candidate, cannot describe baryon asymmetry of the Universe, *etc.* The recently discovered 125 GeV scalar has properties very close to those predicted by the SM. But how close? As long as other new particles are not seen at the LHC, the only relevant BSM models are those allowing for the SM-like scenario, *i.e.*, with an SM-like Higgs boson and other new particles too heavy or too weakly interacting to be observed in the existing experiments.

The main production channel of the Higgs particle at the LHC is the gluon–gluon fusion. The channels allowing most precise measurements are Higgs decays to $\gamma\gamma$ and ZZ. Loop couplings of the Higgs to gauge bosons gg, $\gamma\gamma$, γZ are sensitive to new physics (even to contribution of very heavy particles due to non-decoupling effects). The overall signal strength is equal to $\mu = 1.00 \pm 0.13$ (CMS) [4], $1.30 \pm 0.12(\mathrm{stat})^{+0.14}_{-0.11}(\mathrm{syst})$ (ATLAS) [5].

1.3. Dark Matter

Throughout the years much evidence for the existence of DM has been collected: rotation curves of galaxies, gravitational lensing, *etc.* [8]. A typical candidate for DM is the so-called WIMP (weakly interacting massive particle). The DM relic density is inferred from the measurements made by WMAP and Planck with a good accuracy [9]. There are other astrophysical experiments searching for DM, either directly (via scattering off nuclei) or indirectly (search for products of DM annihilation or decay). Unfortunately, the picture given by these experiments is not entirely consistent. However, some information about DM can be drawn from the LHC measurements, and hopefully it can shed some light on its nature.

2. Inert Doublet Model

Among the simplest extensions of the Higgs sector in the SM are models with two SU(2) doublets (Two Higgs Doublet Models — 2HDMs). In the non-supersymmetric type of the 2HDMs, a special role is played by the Inert Doublet Model (IDM) — the only version of 2HDM with a stable particle (scalar) [10, 11].

In the IDM, the scalars' interactions are defined by the following potential

$$V = -\frac{1}{2}\left[m_{11}^2\left(\phi_S^\dagger\phi_S\right) + m_{22}^2\left(\phi_D^\dagger\phi_D\right)\right] + \frac{1}{2}\left[\lambda_1\left(\phi_S^\dagger\phi_S\right)^2 + \lambda_2\left(\phi_D^\dagger\phi_D\right)^2\right]$$
$$+\lambda_3\left(\phi_S^\dagger\phi_S\right)\left(\phi_D^\dagger\phi_D\right) + \lambda_4\left(\phi_S^\dagger\phi_D\right)\left(\phi_D^\dagger\phi_S\right) + \frac{1}{2}\lambda_5\left[\left(\phi_S^\dagger\phi_D\right)^2 + \left(\phi_D^\dagger\phi_S\right)^2\right]. \tag{1}$$

This potential possesses a global discrete $\mathbb{Z}_2$-type symmetry D under action of which the field ϕ_D changes sign, while ϕ_S remains untouched. The interactions with fermions are chosen in the IDM such as to preserve this symmetry, *i.e.*, only ϕ_S couples to fermions. In this way, the whole IDM Lagrangian is D-symmetric, and moreover, the vacuum state of this model is such that D is not broken spontaneously. The VEVs of the two doublets read

$$\langle\phi_S\rangle = \begin{pmatrix} 0 \\ \frac{v_S}{\sqrt{2}} \end{pmatrix}, \qquad \langle\phi_D\rangle = \begin{pmatrix} 0 \\ 0 \end{pmatrix}. \tag{2}$$

With these choices, the model possesses an exact D-symmetry, which leads to a conserved quantum number (D parity). Because of that, the lightest D-odd particle is stable, and constitutes a good candidate for a DM particle.

The particle spectrum of the IDM consists of the Higgs boson h which follows from the ϕ_S doublet, and the dark scalars H, A and $H^\pm$ coming from ϕ_D. The Higgs boson h has all tree-level couplings to fermions and gauge bosons equal to the SM ones. Nonetheless, some non-SM effects can occur at the loop level, due to the existence of new scalars. The dark scalars do not couple to fermions at the tree level but they do interact with the gauge bosons (through the covariant derivative) and the Higgs particle. The lightest among them that is neutral one plays the role of the DM particle. Here, we assume that $M_H < M_A, M_{H^\pm}$, hence H is the DM candidate in our model.

Deviations from the SM properties of the Higgs boson can be observed in two ways, because of decays of the Higgs to invisible dark particles or because of the additional loop effects thereof. In the following, we will first discuss the invisible decays of the Higgs boson, and then the loop induced decays of the Higgs boson to a pair of photons.

2.1. Invisible Higgs decays

The Higgs boson of the IDM, apart from the SM decay channels, has additional ones to dark particles: $h \to AA, HH$ or $H^\pm H^\mp$. The last channel is excluded (at the tree-level) by the LEP limits for $M_{H^\pm}$: $M_{H^\pm} \gtrsim 70$ GeV. The partial decay width for the process $h \to HH$ reads (see *e.g.* Ref. [19])

$$\Gamma(h \to HH) = \frac{\lambda_{345}^2 v^2}{32\pi M_h} \sqrt{1 - \frac{4M_H^2}{M_h^2}}, \tag{3}$$

where $\lambda_{345} = \lambda_3 + \lambda_4 + \lambda_5$ is the coupling between the Higgs boson and a pair of DM particles. For the decay $h \to AA$, the parameters λ_{345} and M_H have to be replaced by $\lambda_{345}^- = \lambda_3 + \lambda_4 - \lambda_5$ and M_A, respectively.

Since the decay width (3) depends on the mass of the product of the decay and its coupling to the Higgs boson, these quantities can be constrained with the use of the LHC results on the branching ratio of the Higgs boson decay to invisible particles. In the same way, the measurement of the total Higgs decay width can be used, since $\Gamma(h \to \text{inv})$ contributes significantly to it (see the next section). Below, for the sake of simplicity, we will assume that A is too heavy for the $h \to AA$ process to be allowed, *i.e.*, $M_H < M_h/2$ and $M_A > M_h/2$. In Fig. 1 the constraints on λ_{345} and M_H, coming from the experimental constraints on $\text{Br}(h \to \text{inv}) < 0.37$ [12] and on the total width $\Gamma(h) < 5.4\ \Gamma(h)^{\text{SM}}$ [13], are presented. From Fig. 1 one can see that the coupling λ_{345} is constrained by $\text{Br}(h \to \text{inv})$ to a small value, $|\lambda_{345}| \lesssim 0.05$ for $M_H < 62$ GeV.

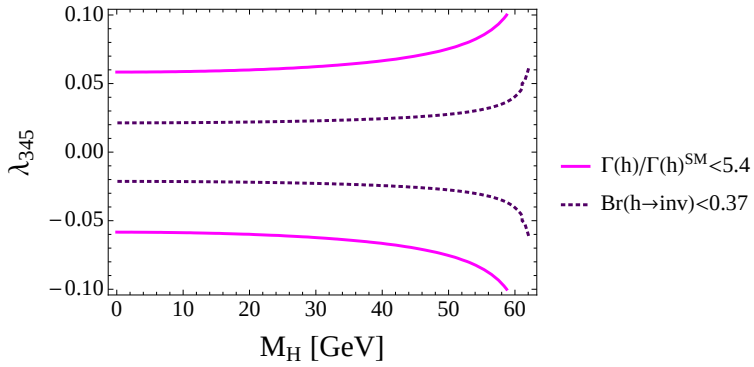


Fig. 1. Constraints on λ_{345} and M_H following from the LHC measurement of $\mathrm{Br}(h \to \mathrm{inv})$ and $\Gamma(h)$. The region between the corresponding curves is allowed. We assume that the decay $h \to AA$ is kinematically forbidden.

2.2. Higgs decays to $\gamma\gamma$

The differences between the SM and the IDM can also be observed in the loop induced decays of the Higgs boson, $h \to \gamma\gamma$ and $h \to Z\gamma$. The first of these decays, being measured very precisely, gained recently much attention, since the first measurements showed some deviation from the SM expectation giving a hint on the existence of new physics. Nowadays, these measurements came closer to the SM, as the observed signal strengths (often denoted by $\mu_{\gamma\gamma}$) are $R_{\gamma\gamma} = 1.17 \pm 0.27$ (ATLAS) [14], $1.14^{+0.26}_{-0.23}$ (CMS) [15], where the expectation of the SM is $R_{\gamma\gamma} = 1$. We see that still new physics effects are acceptable within the experimental bounds. Note that the $Z\gamma$ signal strength has not yet been measured with enough precision to constrain new physics.

Let us consider $R_{\gamma\gamma}$ for the 125 GeV-h in the IDM (see *e.g.* Refs. [16–18])

$$R_{\gamma\gamma} := \frac{\sigma(pp \to h \to \gamma\gamma)^{\mathrm{IDM}}}{\sigma(pp \to h \to \gamma\gamma)^{\mathrm{SM}}} \approx \frac{\mathrm{Br}(h \to \gamma\gamma)^{\mathrm{IDM}}}{\mathrm{Br}(h \to \gamma\gamma)^{\mathrm{SM}}}\,, \tag{4}$$

where we have used the narrow-width approximation and the fact that the main production cross section $gg \to h$ is in the IDM the same as in the SM.

In the formula above $\mathrm{Br}(h \to \gamma\gamma)^{\mathrm{SM}}$ is known, and $\mathrm{Br}(h \to \gamma\gamma)^{\mathrm{IDM}} = \Gamma(h \to \gamma\gamma)^{\mathrm{IDM}}/\Gamma(h)^{\mathrm{IDM}}$. All the tree-level decay widths of the Higgs boson to SM particles are in the IDM the same as in the SM. Only the existence of the invisible decay channels, and the $\gamma\gamma$ and $Z\gamma$ decays can modify the total decay width. However, the branching ratios of the latter are very small, of the order of 10^{-3}–10^{-2} so they can be ignored, and to a good approximation, only the invisible channels modify $\Gamma(h)$ (we used this fact already in Sec. 2.1). The branching ratios in the IDM are presented in Fig. 2

as functions of λ_{345}. Note that once the invisible channels are kinematically allowed, they dominate over the SM channels, so, in general, they tend to suppress $R_{\gamma\gamma}$.

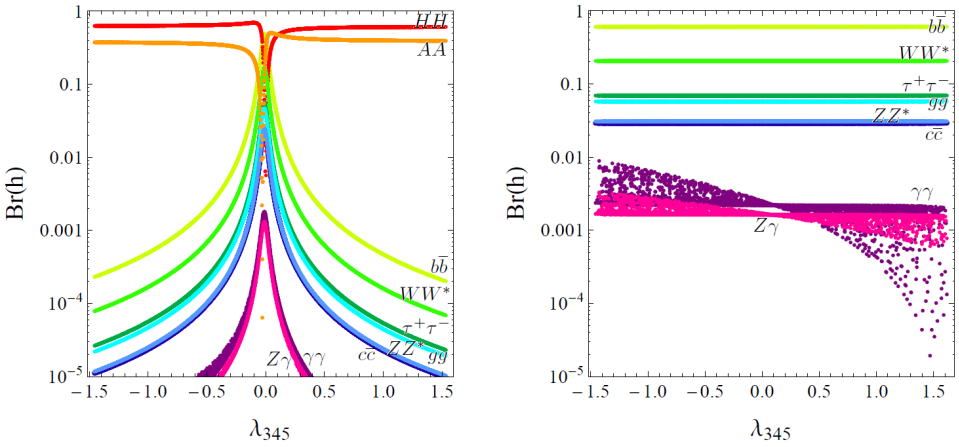


Fig. 2. Branching ratios of the Higgs boson in the IDM as functions of λ_{345}. Left: invisible channels open ($M_H = 50$ GeV, $M_A = 58$ GeV). Right: invisible channels closed ($M_H = 75$ GeV, $M_A > M_H$). From Ref. [16].

If invisible channels are closed, the partial decay width $\Gamma(h \to \gamma\gamma)$, although small, can be a valuable source of information. In the SM, the $h \to \gamma\gamma$ decay is induced by the $W^{\pm}$ boson loop and fermionic loops (the top quark dominates). In general, in the IDM $\Gamma(h \to \gamma\gamma)$ differs from the SM one because of an extra contribution due to the charged scalar, $H^{\pm}$. This contribution can interfere either constructively or destructively with the SM part. Already in Fig. 2 (right panel), it is visible that $\mathrm{Br}(h \to \gamma\gamma)$ can be enhanced or suppressed with respect to the SM.

2.2.1. Enhanced diphoton signal strength

Let us first analyse the consequences of enhanced signal strength (we follow Ref. [16]). In the left panel of Fig. 3, the dependence of $R_{\gamma\gamma}$ on M_H is shown. One can clearly see that for $M_H < M_h/2 \approx 62.5$ GeV, the diphoton signal strength is always suppressed with respect to the SM. This means that if enhancement of the $R_{\gamma\gamma}$ is observed, DM with mass below 62.5 GeV is excluded.

In the right panel of Fig. 3, the allowed $(m_{22}^2, M_{H^{\pm}})$ region, obtained by scanning the parameter space subject to relevant theoretical and experimental constraints[1], is presented. The parameter m_{22}^2 is important for $R_{\gamma\gamma}$

[1] Such as perturbative unitarity, stability of the inert vacuum as well as the LEP limits and the EW precision data (S, T parameters).

because the coupling between the Higgs boson and the charged scalar is proportional to $2M_{H^\pm}^2 + m_{22}^2$. In the region marked by gray/light green $R_{\gamma\gamma} > 1$, while the lines (purple) indicate constant values of $R_{\gamma\gamma}$. Note that for $R_{\gamma\gamma} \geq 1$, the viable region is unconstrained, however for substantial enhancement of $R_{\gamma\gamma}$, the allowed region is bounded. For example, for $R_{\gamma\gamma} > 1.2$, only fairly light charged scalar (and since $M_H < M_{H^\pm}$ also DM) are allowed, $M_{H^\pm}, M_H \lesssim 154$ GeV. The case where $R_{\gamma\gamma}$ goes below 1 will be analysed in the next section, and combined with the DM astrophysical measurements.

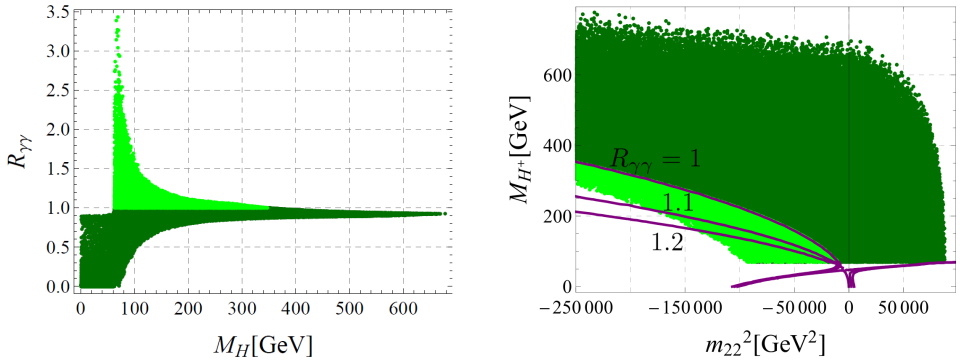


Fig. 3. Left: $R_{\gamma\gamma}$ dependence on M_H. Right: region allowed by the experimental and theoretical constraints in the $(m_{22}^2,\ M_{H^\pm})$ plane. Gray/light green indicates the region where $R_{\gamma\gamma} \geqslant 1$, the lines correspond to the constant values of $R_{\gamma\gamma}$. Plots are made for -25×10^4 GeV$^2 \leqslant m_{22}^2 \leqslant 9 \times 10^4$ GeV^2. From Ref. [16].

2.3. DM constraints from the Higgs LHC and Planck data

The current Planck 3σ limit for DM relic density is $0.1118 < \Omega_{\rm DM}h^2 < 0.1280$ [9]. $\Omega_{\rm DM}h^2$ depends on DM annihilation and production channels, so this measurement constrains the mass and the couplings of the DM candidate. The IDM is a so-called "Higgs-portal" DM model, *i.e.*, in a wide range of masses, the DM candidate couples to fermions mainly through the exchange of h. Therefore, the coupling λ_{345} between the Higgs and the DM candidate is constrained by the relic density measurement. On the other hand, the same coupling as was shown before, is important for the diphoton signal strength. This gives us opportunity to combine these two types of constraints. In the following, we will examine the case $R_{\gamma\gamma} > 0.7$ (with agreement with 3σ LHC limit), we studied other cases in [19].

Figure 4 shows how the constraints arise. In the left panel, $R_{\gamma\gamma}$ as a function of λ_{345} is shown (for fixed values of masses). If we require that $R_{\gamma\gamma} > 0.7$, upper and lower bounds on λ_{345} arise. In the right panel, the

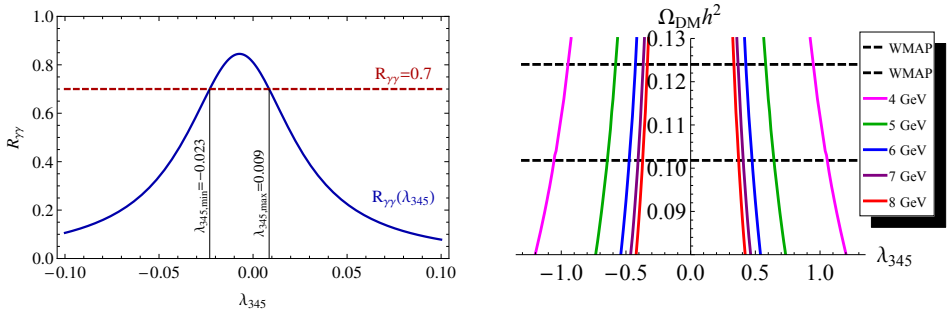


Fig. 4. Left: $R_{\gamma\gamma}$ as a function of λ_{345} for $M_H = 55$ GeV, $M_A = 60$ GeV, $M_{H^\pm} = 120$ GeV (from Ref. [19]). Right: relic density of DM as a function of λ_{345} for different DM mass. The WMAP 3-σ bound is marked by the dashed black horizontal lines (from Ref. [21]).

relic density of the DM as a function of λ_{345} is presented for different values of M_H. To fall within the $\Omega_{\rm DM}h^2$ experimental limits (*i.e.*, between the black dashed horizontal lines)[2] the value of λ_{345} should be between the upper and lower limits. These two types of bounds will be combined in the following.

It has been shown in previous works [20, 21] that the DM in the IDM can have correct relic abundance only in three regions: for very light DM ($M_H \lesssim 10$ GeV), intermediate DM (40 GeV $\lesssim M_H \lesssim 160$ GeV), and heavy DM ($M_H \gtrsim 500$ GeV). We will analyse these cases separately, following Ref. [19].

As can be seen in the right panel of Fig. 4, the right $\Omega_{\rm DM}h^2$ of very light DM is obtained for $|\lambda_{345}| \sim \mathcal{O}(0.5)$. Smaller coupling means that the DM does not annihilate efficiently enough, and the relic abundance is too big. As λ_{345} in agreement with the LHC limit $R_{\gamma\gamma} > 0.7$ is around $|\lambda_{345}| < 0.04$, the two requirements cannot be reconciled, and the very light DM is excluded. Results for intermediate and heavy masses are presented in Fig. 5. The shades (of gray/blue) indicate the values of $R_{\gamma\gamma}$. On this, constraints from Planck are superposed. The dark gray inner region is excluded ($\Omega_{\rm DM}h^2$ is too big). The two idicated by arrows/red bands are in agreement with Planck data (correct relic density), and in the remaining region the relic density is too low (another DM component would be necessary in order to comply with the relic density data). In the left panel, a plot for intermediate DM, with $M_H < M_h/2$ is presented. One can see that the relic density constraints (Planck) are in agreement with the assumption $R_{\gamma\gamma} > 0.7$ only for $M_H > 53$ GeV. In the middle panel, intermediate DM with $M_H > M_h/2$ is analysed. Here, all the points that are in agreement with the Planck measurement also give $R_{\gamma\gamma} > 0.7$. However, if Planck constraints are to be

[2] In this illustrative plot, the WMAP limits are presented but later on we will use the more accurate Planck results.

met, no enhancement in $R_{\gamma\gamma}$ is possible. For the heavy DM (right panel of Fig. 5), we can get correct relic density for all values of masses. Note that $R_{\gamma\gamma}$ is very close to 1 for this case.

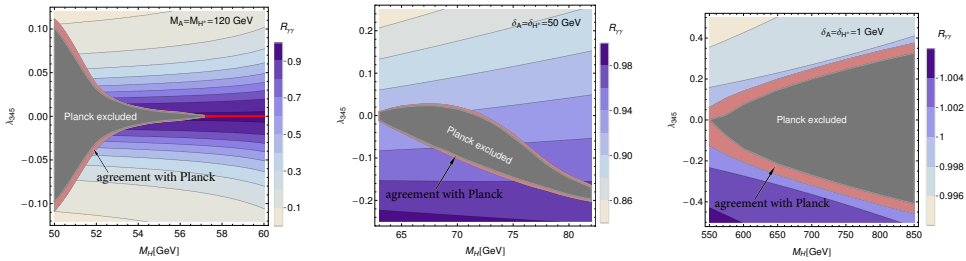


Fig. 5. Maps of the $R_{\gamma\gamma}$-values in the $(M_H,\ \lambda_{345})$ plane for the intermediate DM with $h \to HH$ channel open (left), $h \to HH$ channel closed (middle), and for heavy DM (right) in comparison with the allowed by Planck (red) bands.

2.4. Comparison with direct DM detection experiments

The constraints obtained above can be compared with the results of the direct experimental search of the DM [19], where the DM is supposed to scatter off the nuclei. In the Higgs-portal models, among them IDM, the cross section $\sigma_{\mathrm{DM},N}$ is proportional to the square of the coupling of Higgs to DM (λ_{345}^2) because the DM interacts with the nucleus through the exchange of the Higgs boson, $\sigma_{\mathrm{DM},N} \sim \lambda_{345}^2 f_N^2/(M_N+M_H)^2$, where f_N is a formfactor, and M_N is the mass of the nucleon. In Fig. 6, a comparison of our results

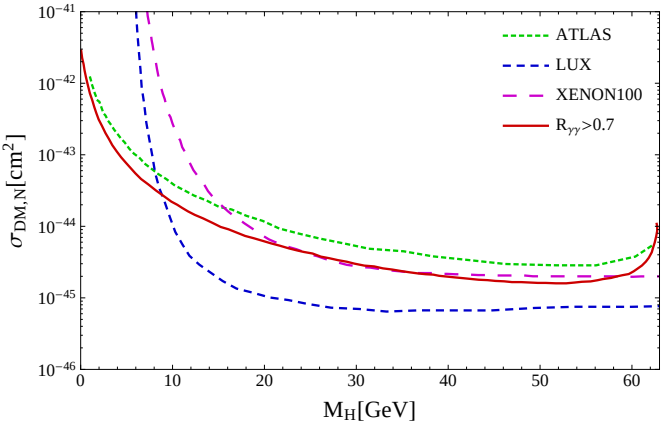


Fig. 6. Our results for upper limits on $\sigma_{\mathrm{DM},N}$ coming from the limit $R_{\gamma\gamma} > 0.7$ (and $f_n = 0.326$) compared with upper limits from LUX and XENON100 experiments, and from the LHC constraints (ATLAS) on the Higgs invisible Br.

coming from the limit $R_{\gamma\gamma} > 0.7$, and the constraints from direct DM search experiments (LUX and XENON100), and from the constraints on invisible Higgs branching ratio (LHC ATLAS) are presented. Note, that our upper limits, represented by the line $R_{\gamma\gamma} > 0.7$, are competitive with the upper limits from the mentioned dedicated DM experiments.

Similarly, the constraints coming from the DM relic density measurements (medium gray/red bands in Fig. 5) can be translated to constraints on the DM–nucleon scattering cross section. In Fig. 7 the allowed regions of $\sigma_{\mathrm{DM},N}$ (dark gray/red bands) as a function of M_H are shown. They are coming from λ_{345} regions allowed by the Planck data and $R_{\gamma\gamma} > 0.7$ ($f_N = 0.326$). Comparison with upper limits from LUX is shown. We see that the direct detection limits (LUX) stay in agreement with these constraints [22], however loop corrections can bring the model close to the future experiments reach [23].

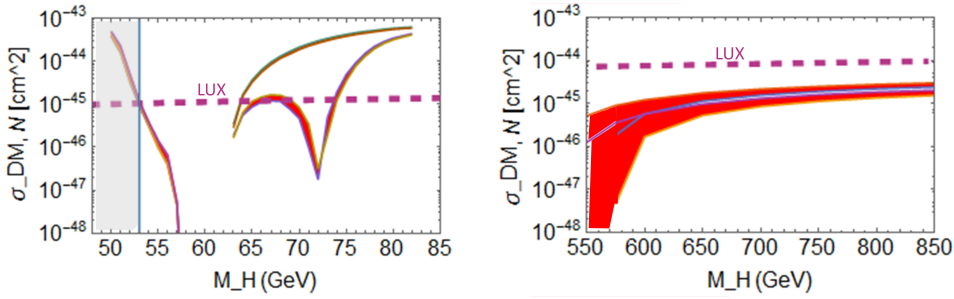


Fig. 7. Allowed regions of $\sigma_{\mathrm{DM},N}$ coming from the Planck limit on the DM (dark gray/red bands), compared with upper limits from LUX (and $f_N = 0.326$). For lower mass, part of allowed regions ($M_H < 53$ GeV) are excluded by $R_{\gamma\gamma} > 0.7$ condition.

3. Conclusions

The discovery of the Higgs boson was awaited for a long time since it was the last component needed to complete the Standard Model. Moreover, it also opens door to exploration of new phenomena. Search for new particles at the LHC gives exciting perspectives, but we can also use the available data, *e.g.*, the measurements of the Higgs boson properties, especially the $\gamma\gamma$ signal strength, to shed light on such issues as the properties of the DM. Other dedicated analysis of the DM in the IDM are ongoing, *e.g.* on the lepton pair production at the LHC in the processes $q\bar{q} \to HA$ followed by $A \to HZ$ or $H \to l\bar{l}$ [24]. Finally, models like IDM can shed some light also on the problem of the thermal evolution of the Universe [25].

This article is based on a presentation given by M. Krawczyk at the Applied Nuclear Physics and Innovative Technologies 2014 Symposium. M.K. would like to thank organizers of this interesting symposium for invitation, warm hospitality and exceptional atmosphere. We thank P. Swaczyna for his contribution to this work. The work of M.K. and D.S. was partially supported by the grant NCN OPUS 2012/05/B/ST2/03306 (2012–2016). The work of B.Ś. was supported by the Polish National Science Centre grant PRELUDIUM, under the decision number DEC-2013/ 11/N/ST2/04214.

REFERENCES

[1] F. Englert, R. Brout, *Phys. Rev. Lett.* **13**, 321 (1964).
[2] P.W. Higgs, *Phys. Lett.* **12**, 132 (1964); *Phys. Rev. Lett.* **13**, 508 (1964); *Phys. Rev.* **145**, 1156 (1966).
[3] G.S. Guralnik, C.R. Hagen, T.W.B. Kibble, *Phys. Rev. Lett.* **13**, 585 (1964).
[4] The CMS Collaboration, CMS-PAS-HIG-14-009 (2014).
[5] The ATLAS Collaboration, ATLAS-CONF-2014-009 (2014).
[6] G. Belanger *et al.*, *Phys. Lett.* **B723**, 340 (2013).
[7] The ATLAS Collaboration, *Phys. Rev. Lett.* **112**, 201802 (2014).
[8] A. Morselli, Experimental Astroparticle Physics talk at CORFU 2014.
[9] The Planck Collaboration, `arXiv:1303.5076 [astro-ph]`.
[10] N.G. Deshpande, E. Ma, *Phys. Rev.* **D18**, 2574 (1978).
[11] R. Barbieri, L.J. Hall, V.S. Rychkov, *Phys. Rev.* **D74**, 015007 (2006).
[12] The ATLAS Collaboration, ATLAS-CONF-2014-010 (2014).
[13] The CMS Collaboration, *Phys. Lett.* **B736**, 64 (2014).
[14] The ATLAS Collaboration, CERN-PH-EP-2014-198 (2014).
[15] The CMS Collaboration, *Eur. Phys. J.* **C74**, 3076 (2014).
[16] B. Świeżewska, M. Krawczyk, *Phys. Rev.* **D88**, 035019 (2013).
[17] P. Posch, *Phys. Lett.* **B696**, 447 (2011).
[18] A. Arhrib, R. Benbrik, N. Gaur, *Phys. Rev.* **D85**, 095021 (2012).
[19] M. Krawczyk, D. Sokołowska, P. Swaczyna, B. Świeżewska, *J. High Energy Phys.* **1309**, 055 (2013).
[20] E.M. Dolle, S. Su, *Phys. Rev.* **D80**, 055012 (2009); L. Lopez Honorez, E. Nezri, F.J. Oliver, M. Tytgat, *J. Cosmol. Astropart. Phys.* **02**, 028 (2007).
[21] D. Sokołowska, `arXiv:1107.1991 [hep-ph]`.
[22] A. Goudelis, B. Herrmann, O. Stål, *J. High Energy Phys.* **1309**, 106 (2013).
[23] M. Klasen, C.E. Yaguna, J.D. Ruiz-Alvarez, *Phys. Rev.* **D87**, 075025 (2013).
[24] P. Swaczyna, M.Sc. Thesis, University of Warsaw, 2013.
[25] I. Ginzburg *et al.*, *Phys. Rev.* **D82**, 123533 (2010).